Filter Design for Cable Overvoltage and Power Loss Minimization in a Tidal Energy System With Onshore Converters

Filter Design for Cable Overvoltage and Power Loss Minimization in a Tidal Energy System with Onshore Converters

Marios C. Sousounis, Jonathan K.H. Shek, and Markus A. Mueller

***Abstract*—By moving the back-to-back AC-DC-AC converters in a tidal current conversion system onshore, maintenance requirements and cost are reduced significantly. This is because underwater components are not easily accessible and operate in a harsh environment. In addition to increased maintainability, the concept of long distance controls offers maximum power capture from the tidal currents in the same way that a converter in the nacelle would offer. However, a number of challenges are associated with the concept of controlling electrical machines through long cables, which include electromagnetic travelling waves in the cables and system resonance. These phenomena can induce overvoltages at the generator terminals which can lead to system failure and high harmonics that can induce extra power losses. The major contribution of this paper is a new method of filter design, for systems with long distance controls, for minimization of system power loss. The proposed method is validated by developing a full resource-to-grid tidal current conversion system in MATLAB/Simulink. Simulation results show that using the proposed method overvoltage mitigation can be achieved the same way as literature based filters but at the same time minimize the total system losses. The results from the analysis can be used to optimize tidal energy conversion systems with a similar electrical configuration.**

***Index Terms*—Filter design, tidal power generation, overvoltage protection, electromagnetic transient analysis, variable speed drives, harmonic analysis, power transmission.**

I. Introduction

THE world's tides have the potential to generate carbon free energy and contribute to energy sustainability and security. The UK alone has a significant tidal current energy resource which can supply 29% of the UK electricity demand [1]. Tidal energy developers have started to move from single devices usually rated at 1MW – 2MW to small scale demonstration arrays rated at around 10MW. These tidal current conversion systems (TCCS), regardless of technology, require continuous reliable underwater operation with high availability. This dictates that onsite visits must be reduced to a minimum since tidal devices are installed at locations with high tidal currents where the windows of opportunity for site visits are relatively short. Another aspect of tidal arrays that affects power transmission is that devices will be close enough to shore, thereby eliminating equipment which would normally be installed offshore. This consequently minimizes offshore maintenance. In this context, it is suggested that tidal energy developers can improve the availability of their systems by moving the power electronics from the nacelle to the shore. This can reduce offshore visits since the failure frequency of power converters can be significant based on data from onshore wind turbines [2]. Locating the power electronics on land means that the generator has to be controlled via long subsea cables and therefore long distance controls are needed. A block diagram of the TCCS utilizing long distance controls can be seen in Fig. 1.

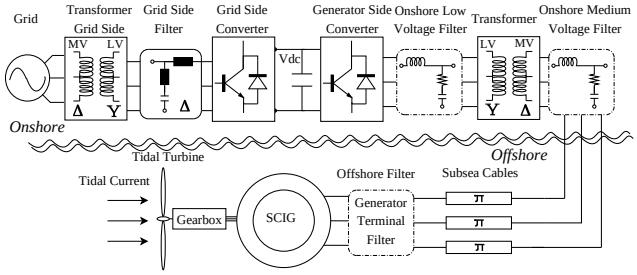

Fig. 1. Block diagram of the complete TCCS model. The three possible positions where the system filter can be installed are depicted. These are the offshore filter, the onshore medium voltage filter and the onshore low voltage filter.

The literature regarding long distance drives focuses on the presence of overvoltages at the terminals of electrical machines with long feeders due to electromagnetic travelling waves. In order to mitigate the overvoltages in these systems research papers focus on different types of passive filters [3 - 6]. In [3] three different types of filters, installed at the machine terminals, are designed and compared and in [4-5] a 2nd-order filter at the inverter output is proposed. Authors in [6] study and compare the effectiveness of filters at the machine terminals and inverter output with respect to filter losses, changes in cable parameters and controller response. Another aspect of research related to long distance controls is system resonance which can induce extreme harmonics and overvoltages. In order to study the resonance between the transformer, the cables and the machine, high-frequency

Manuscript received September 25, 2014; revised February 12, 2015. This work was supported in part by Andritz Hydro Hammerfest and in part by the University of Edinburgh.

The authors are with the Institute for Energy Systems, School of Engineering, The University of Edinburgh, The King's Buildings, Mayfield Road, Edinburgh, EH9 3JL, United Kingdom (e-mail: M.Sousounis@ed.ac.uk).

modeling is required [7-9]. Finally, in [10] an in-depth analysis is given regarding the design of a 2nd-order filter at the inverter output in a TCCS without transformer to mitigate overvoltages due to electromagnetic travelling waves.

Currently, a number of different TCCS configurations exist as tidal developers are trying to improve their concepts. While most of the designs are bottom mounted with horizontal axis rotors and low solidity blades, there are differing approaches in generator technology. Research regarding tidal systems focuses on power limitation mechanisms [11], power capture maximization control methods, generator technologies [12-14] and grid integration [15].

The paper has the following structure. First, the theoretical background regarding the electromagnetic travelling waves in the cables and system resonance is briefly explained in sections II and III respectively. In addition, in section III a way to quantify system resonance is established mathematically. In section IV different parts of the TCCS model are presented. Section V compares the literature-based design process of different types of filters with a proposed filter design process based on voltage gain calculations. Section VI demonstrates and compares results from simulating the system model under different cases. Conclusions derived from the results are summarized in section VII.

II. Wave Reflection Analysis

Voltage pulses, created by the generator side controller, travel from the VSC to the generator through the cables. Their behavior can be analyzed the same way as travelling waves in transmission lines [3]. Voltage waves travelling from the VSC to the generator are reflected at the end of the long cables. The voltage reflection coefficient, Γ_n, is determined by the surge impedance ratio at node n.

$$\Gamma_n = \frac{Z_n - Z_C}{Z_n + Z_C} \tag{1}$$

Where Z_C is the cable characteristic impedance at specified frequency, ω in rad/s, and Z_n is the impedance at node n.

$$Z_C = \sqrt{\frac{(j \cdot \omega \cdot L_C + R_C)}{(j \cdot \omega \cdot C_C)}} \tag{2}$$

The impedance at the VSC terminals is very low because it is dominated by the dc-link capacitor and therefore results in $\Gamma_{VSC} \approx -1$. According to [3] the surge impedance of the generator is very high for low power machines but for high power machines this can be less than 0.65 [4]. In this paper, two cases will be explored regarding the generator surge impedance. Firstly, a worst case scenario is chosen where the travelling waves arriving at the generator terminals are completely reflected resulting in 2 times the voltage magnitude of the travelling waves. Based on (1) this leads to $\Gamma_{Gen} \approx 1$. The second scenario assumes a voltage reflection coefficient at the generator terminals equal to $\Gamma_{Gen} = 0.5$ which means that the travelling waves arriving at the generator terminals are reflected by 50% resulting in 1.5 times the voltage magnitude of the travelling wave. When designing filters only the worst-case scenario will be taken into account. Results regarding the two scenarios are given in section VI. Fig. 2 shows the voltage waveform at the generator terminals for the proposed TCCS when filters are not designed properly.

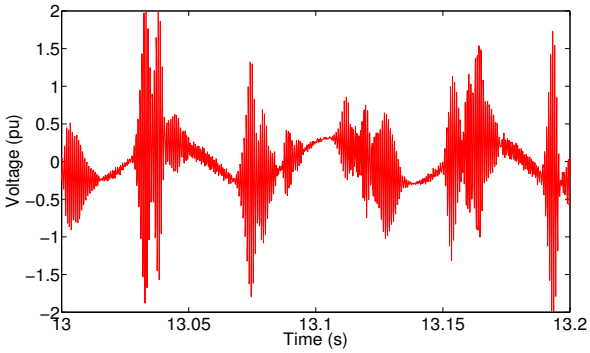

Fig. 2. Voltage waveform at the generator terminals for the TCCS under consideration when filters are not designed properly. Voltage peaks up to 2pu appear. The maximum allowable overvoltage is 1.2pu.

III. System Resonance

Apart from the voltage reflections, additional overvoltages can be generated by the interaction of cable capacitance and inductance. This interaction creates frequencies where the system is resonant [4]. If harmonics are generated at the resonant frequencies then these harmonics can be magnified and lead to overvoltages and increased harmonic distortion at the generator terminals. In addition, when a transformer is installed between the VSC and the cables, transformer inductance interacts with cable capacitance creating additional resonant frequencies. In order to quantify the phenomenon of resonance, voltage gain graphs where created for the cables in isolation and also cables with the transformer as a system, as shown in Fig. 3. The voltage gain graph is created by assuming that the VSC is sending voltage pulses and that the generator terminals are the receiving end of these pulses. Therefore we can compute the state-space model of the system using MATLAB in discrete form:

$$\begin{aligned} x(kT+T) &= Ax(kT) + Bu(kT) \\ y(kT) &= Cx(kT) + Du(kT) \end{aligned} \tag{3}$$

Where T is the sampling interval, kT is the time instant, input vector x represents inductor currents and capacitor voltages, input vector u represent voltage and current sources and output vector y represents voltage and current measurements. So, in order to create the voltage gain graph, (3) is simplified to:

$$\begin{aligned} x(kT+T) &= Ax(kT) + B \cdot V_{VSC}(kT) \\ V_{Gen}(kT) &= Cx(kT) + D \cdot V_{VSC}(kT) \end{aligned} \tag{4}$$

Manipulating (4) the voltage gain graph can be expressed as in (5).

$$V_{GAIN}(s) = \frac{V_{Gen}(s)}{V_{VSC}(s)} \tag{5}$$

The magnitude of the voltage gain graph shows how each frequency component of the voltage pulses generated are multiplied to reach the generator. Therefore, if there is a significant harmonic component generated at a frequency where the voltage gain magnitude is above unity, then this harmonic component will be magnified at the generator

terminals. On the other hand, if the voltage gain is below unity at a specific frequency range then the harmonic components at these frequencies will be reduced at the generator terminals. The magnitude of the voltage gain graph and where magnitude peaks appear are directly related to cable and transformer parameters. The voltage gain graph can be seen in Fig. 3.

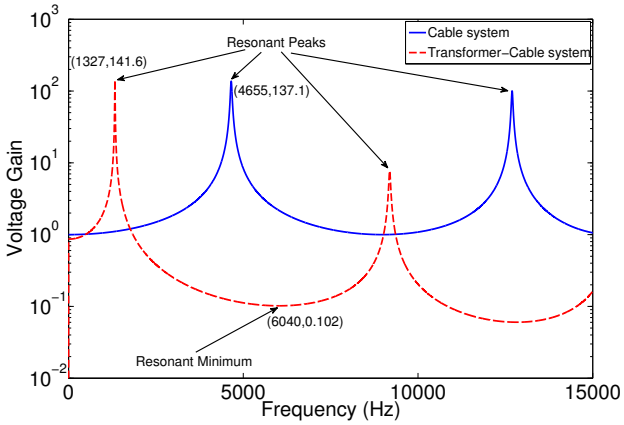

Fig. 3. Voltage gain graph for a system with cables only and for a system with cables and transformer. There is a significant change in resonant frequencies when the transformer is included in the analysis.

IV. Modeling of the Proposed TCCS

In this section the modeling aspects of the TCCS will be described. The proposed topology can be seen in Fig. 1. The power output of the medium voltage generator is transmitted to shore by long three-phase subsea cables. The medium voltage is transformed to low voltage using an onshore transformer. The generator-side converter is controlled by the DTC SVM method which allows the SCIG to operate with variable speed. On the grid side, the low voltage output of the inverter is first filtered and then a step-up transformer is used in order to match the high voltage of the grid. The modeling aspects of this system are described in [17]. In this paper cable and flow modelling will be described in more depth.

A. Tidal Resource

The power potential of a tidal turbine can be derived by the same formulas as for wind energy systems:

$$P_{Tide} = \frac{1}{2} \cdot \rho_{water} \cdot Cp(\lambda, \beta) \cdot A \cdot V_{current}^{3} \tag{6}$$

where ρ_{water} is the sea water density approximately equal to 1025kg·m^{-3}, A is the swept area by the tidal turbine blades, $V_{current}$ is the fluid speed in m/s, power coefficient Cp, tip speed ratio λ and pitch angle β in degrees.

For the purposes of this study the input flow speed is chosen to be above 2m/s as we intend to study the operation of the system at rated conditions. The mean flow speed comes from measured data in which a predicted turbulence of 10% and swell effects were added. The predicted turbulence is modelled by adding white noise to the measured mean flow speed. The swell effect of the tides was considered in the resource model using a first-order Stokes model as described in [15-16]. Therefore, the tidal flow is composed of three distinct parts, the mean flow speed, the turbulence and the swell effect. The flow speed is given in (7) and the flow generated is shown in Fig. 4.

$$V_{tide}(t) = V_{mean}(t) + V_{turbulence}(t, P) + V_{Swell}(t, z, x) \tag{7}$$

Where P is the noise level, z is the vertical point for the swell and x is the horizontal point for the swell.

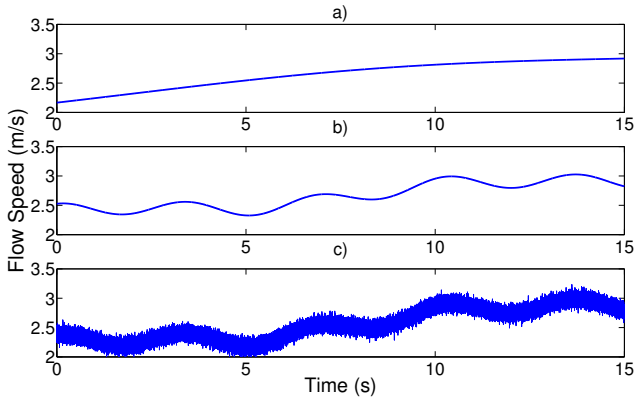

Fig. 4. Tidal current speed used as input to the model. First plot shows the mean flow speed (a). The second plot shows the flow speed when the swell effect is considered (b). The third plot shows the flow speed with swell effect and turbulence (c).

B. Cable Modeling

In this paper we have chosen to model the long subsea cables with a network of π-sections. In a transmission cable, the resistance R_C, the inductance L_C and the capacitance C_C are uniformly distributed along the cable. In order to accurately represent the uniform distrubution with lumped parameters and therefore obtain accurate results at the cable terminals for transient analysis, several identical π-sections are connected in series. The number of these identical π-sections depends on cable parameters, cable length (l_C) and the frequency range which must be accurately represented (f_{max}). An approximation of the number of π-sections required to accurately represent frequency transients is given by the following equation:

$$N = \frac{8 \cdot l_C \cdot f_{\max}}{v_C} \tag{8}$$

Where v_C is the travelling speed of the waves in the cables and is defined in (9).

$$v_C = \frac{1}{\sqrt{L_C \cdot C_C}} \tag{9}$$

For the purposes of this paper, the analysis has been performed by assuming a cable length that is suitable for most tidal energy projects. In addition, the transient analysis of this system lies in the low frequency range and therefore f_{max} = 5kHz. The parameters of the cascaded π-network are given in Table I and Fig. 5 depicts the cable as modeled.

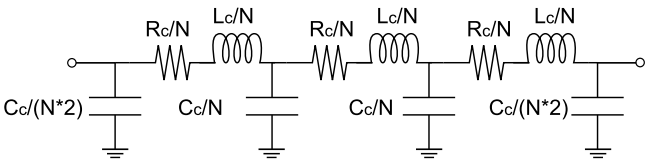

Fig. 5. Modeling the cables for the TCCS. Three π-sections are modeled, N = 3. Resistance, capacitance and inductance are multiplied by the cable length, l_C, to receive their final value.

TABLE I
SUBSEA CABLE NETWORK PARAMETERS

Symbol	Quantity	Value
R_C	Cable resistance per unit length	0.1970 Ω/km
L_C	Cable inductance per unit length	0.742 mH/km
C_C	Cable Capacitance per unit length	0.31 μF/km
l_C	Cable length	3.5 km
Z_C	Cable characteristic impedance	52.5708 - 19.2389·j
N	Number of π-sections	2.12
N`	Number of π-sections chosen[a]	3
f_{max}`	Maximum accurately represented frequency[a]	7000 Hz

[a]Since 2 π-sections cannot represent the frequency range of 5000Hz, we chose 3 π-sections that can actually represent f_{max}.

V. FILTER DESIGN METHODOLOGY

The installation of a filter at the generator side of a tidal energy system with long distance controls must ensure continuous underwater operation, prevent overvoltages and generate the minimum possible losses. At the following sections most filters that appear in the literature regarding long distance controls are discussed and filter parameters are calculated based on the equations provided for the TCCS described above. After calculating the parameters based on the literature, a new method of calculating filter parameters based on the voltage gain graphs is described.

A. Filter parameters based on literature

1) Offshore filter

As described in section II the voltage reflection coefficient at the generator terminals can be calculated using (1). In the worst case scenario Γ_{Gen} = 1 whereas the desirable value for the voltage reflection coefficient at the generator terminals is Γ_{Gen} = 0. Therefore, by terminating the long cables with impedance equal to the cable characteristic impedance we can achieve the desirable value.

a) Resistor Termination

Installing a parallel resistor (R) at the machine terminals is suggested [3] to provide voltage overshoot damping (Fig. 6). In order to achieve this, the resistor value must be equal to the cable characteristic impedance.

$$R_{filter} = |Z_C| = 55.98\,\Omega = Z_{filter} \tag{10}$$

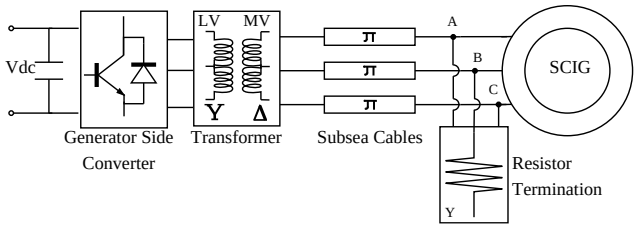

Fig. 6. Block diagram of the generator side TCCS with Resistor Termination connected in wye.

b) Capacitor Resistor Termination

A first-order damped high pass resistor-capacitor (CR) filter at the machine terminals will provide overvoltage mitigation the same way as R [3] but with lower losses (Fig. 7). In order to choose the CR filter values we have to consider that initially the capacitor behaves as a short circuit and therefore [6]:

$$R_{filter} = real(Z_C) = 52.57\,\Omega \tag{11}$$

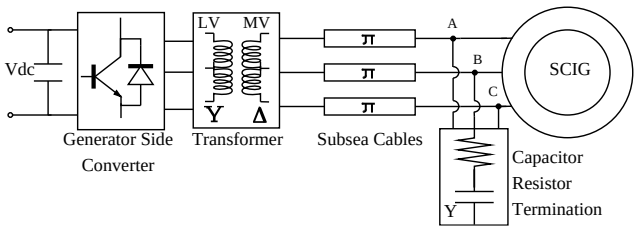

Fig. 7. Block diagram of the generator side TCCS with Capacitor Resistor Termination connected in wye.

Filter capacitance is chosen so that there is less than 20% of terminal voltage during steady state operation [4].

$$C_{filter} = \frac{(-1)\cdot 3\cdot\left(l_c\cdot\sqrt{L_C\cdot C_C}\right)}{2\cdot Z_C\cdot\ln(0.8)} = 6.3741\,\mu F \tag{12}$$

The impedance of the CR filter at the generator terminals:

$$Z_{filter} = \left| R_{filter} + \frac{1}{\left(j\cdot 2\cdot\pi\cdot f\cdot C_{filter}\right)}\right| = 502.14\,\Omega \tag{13}$$

Where f = 50Hz.

c) Capacitor Resistor Inductor Termination

In [3] the second-order damped high-pass filter (CRL) is proposed in order to mitigate the overvoltages at the machine terminals. The filter is shown in Fig. 8. The methodology to calculate filter parameters is similar to the CR filter:

$$R_{filter} = real(Z_C) = 52.57\,\Omega \tag{14}$$

$$C_{filter} = \frac{1}{2\cdot R_{filter}}\cdot\frac{1}{2\cdot\pi\cdot f_{tuned}} = 6.055\,\mu F \tag{15}$$

$$L_{filter} = \frac{1}{C_{filter}}\cdot\left(\frac{1}{2\cdot\pi\cdot f_{tuned}}\right)^2 = 66.9\,mH \tag{16}$$

The capacitance and inductance of the filter are based on the tuned frequency which can be derived by (17):

$$f_{tuned} = \frac{1}{2\cdot\pi\cdot\sqrt{L_{filter}\cdot C_{filter}}} = 250\,Hz \tag{17}$$

The CRL filter impedance can be calculated:

$$Z_{filter} = \left|\frac{1}{\left(j\cdot 2\cdot\pi\cdot f\cdot C_{filter}\right)} + \frac{R_{filter}\cdot j\cdot 2\cdot\pi\cdot f\cdot L_{filter}}{R_{filter} + j\cdot 2\cdot\pi\cdot f\cdot L_{filter}}\right| \tag{18}$$

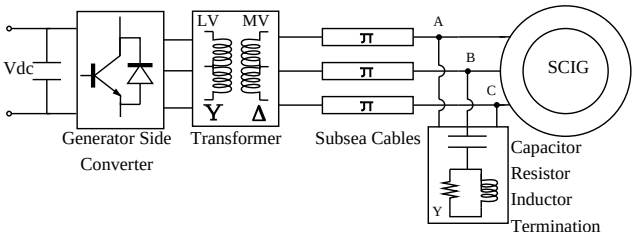

Fig. 8. Block diagram of the generator side TCCS with Capacitor Resistor Inductor Termination connected in wye.

2) Onshore filters

Onshore filters have an advantage over offshore filters in their use for TCCS since they are easily accessible and the operating environment for an onshore filter is friendlier.

a) Medium Voltage LCR Filter

The filter design method of a second-order *LCR* filter for overvoltage mitigation is described in detail in [10] for a converter-cable-generator system:

$$R_{filter} = real\left(Z_C\right) = 52.57\,\Omega \tag{19}$$

$$L_{filter} = R_f \cdot \frac{2 \cdot t_{travel} \cdot \left(\Gamma_{Gen} + 1\right) \cdot \Gamma_{Gen}}{\Delta V_{\max} + 1 + \left(\Gamma_{Gen} - 1\right) \cdot \left(\Gamma_{Gen} + 1\right)} \tag{20}$$

$$C_{filter} = \frac{4 \cdot L_f \cdot \zeta^2}{R_f^2} = 34.31\,\mu F \tag{21}$$

Where ζ = 1.45 is the damping ratio, $\Gamma_{Gen} = 1$ and t_{travel} is the travelling time of the wave front to the receiving end which is calculated from (22).

$$t_{travel} = l_C \cdot \sqrt{L_C \cdot C_C} = 53.08\,\mu s \tag{22}$$

The application of the above filter to the proposed converter-transformer-cable-generator TCCS is shown in Fig. 9. To calculate filter impedance only the parallel RC path is considered which is similar to (13).

$$Z_{filter} = 106.63\,\Omega \tag{23}$$

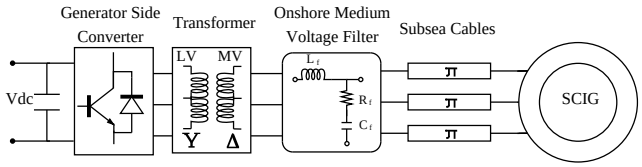

Fig. 9. Block diagram of the generator side TCCS with a medium voltage LCR filter. The LCR filter is composed of an inductor connected in series and a resistor-capacitor branch connected in wye in parallel.

b) Low Voltage LCR Filter

Referring the parameters calculated for the medium voltage LCR filter to the low voltage of the transformer then the LCR filter can be applied at the output of the VSC as shown in Fig. 10. Filter parameters are based on (19) – (21).

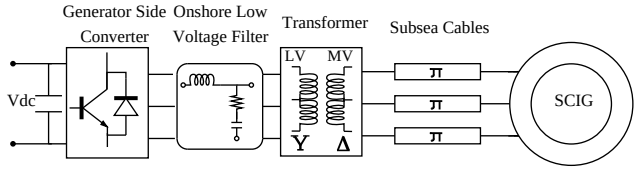

Fig. 10. Block diagram of the generator side TCCS with a low voltage LCR filter. The LCR filter is composed of an inductor connected in series and a resistor-capacitor branch connected in wye in parallel.

B. Filter design algorithm based on voltage gain graph

A new method is proposed for choosing filter values based on the voltage gain graph described in section III. The main aims of the algorithm are to choose filter parameters that:

- Reduce resonant peaks that increase the magnitude of specific harmonics.
- Maximize filter impedance in order to reduce losses induced to the system.

In Fig. 11 we plot the voltage gain graphs of the TCCS when the filters described above are being used. We can observe that the filters installed at the medium voltage side of the system reduce the resonant peaks to very low values. The LCR filter installed at the low voltage side of the transformer does not reduce the resonant peak effectively.

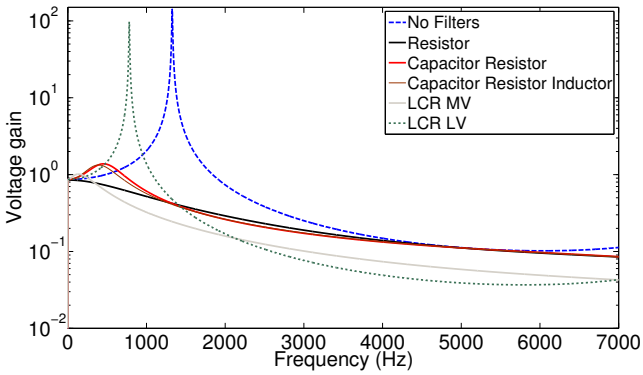

Fig. 11. Voltage gain graph for the TCCS when the different types of filters are installed.

The proposed algorithm for filter design operates in the following way:

1. Reference filter parameters are calculated using filter design equations as described in the literature.
2. A range around the reference parameters is chosen depending on the filter design equations.
3. For a specific set of filter parameters, within the range specified above, the voltage gain graph is computed.
4. The peak value of the voltage gain graph is stored as the worst case overvoltage for that case.
5. Filter impedance is also calculated based on the specific set of parameters chosen in step 3.
6. A new set of filter parameters is chosen and the process is repeated from step 3.

When the algorithm has chosen all the possible sets of filter parameters in step 3, a decision can be made to choose the one that gives better results. In order to quantify and demonstrate the results, contour plots are created in the following sections. The algorithm chooses which set of filter parameters will have better results compared to reference filter parameters by taking into account:

- Peak voltage gain; higher peak can cause increased overvoltages.
- Filter losses; a filter with higher impedance will have lower losses.
- Voltage gain at 50Hz; the higher the voltage gain at 50Hz, the higher the voltage compensation provided by the filter to the generator terminals.

In the next sections, we will show the process to choose a set of filter parameters in detail for the CR filter. For the other filter types, the process is followed in a similar way.

1) Capacitor Resistor Termination (CR)

The block diagram of the CR filter at the machine terminals is shown in Fig. 6. Based on the data acquired by the algorithm a choice can be made for a set of filter values that fulfill the criteria for overvoltage mitigation and power loss reduction. In order to visualize these results we can create a contour graph with the combination of maximum voltage gain and filter impedance.

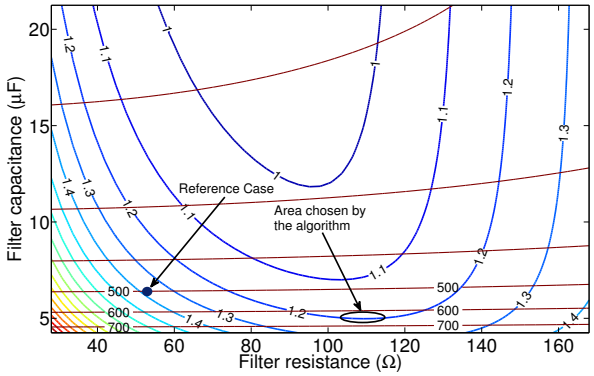

Fig. 12. Filter design graph for the CR filter. The set of parameters the algorithm has chosen are limited by the 1.2 contour line and maximum filter impedance. Reference case maximum voltage gain is 1.382.

2) Resistor Termination (R)

The block diagram for the resistor termination is given in Fig. 6. Since resistor termination has only one variable the filter design graph that appears in Fig. 13 contains the response at each frequency.

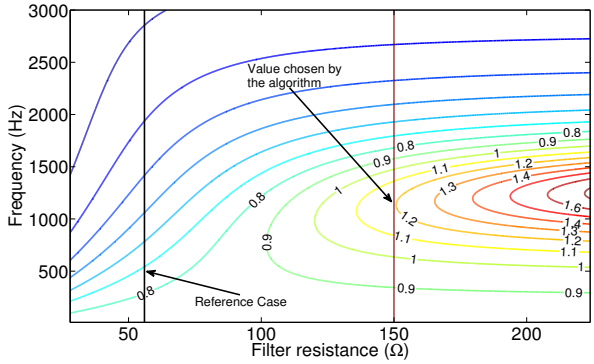

Fig. 13. Filter design graph for the resistor termination. The set of parameters the algorithm has chosen are limited by the 1.2 contour line and the vertical line of filter impedance that is adjacent to this line.

3) Capacitor Resistor Inductor Termination (CRL)

The block diagram for the CRL filter is given in Fig. 8. Based on (15) - (17), by changing f_{tuned} we can obtain the capacitor and inductor values needed to design the filter. Fig. 14 depicts the filter design graph for the CRL filter.

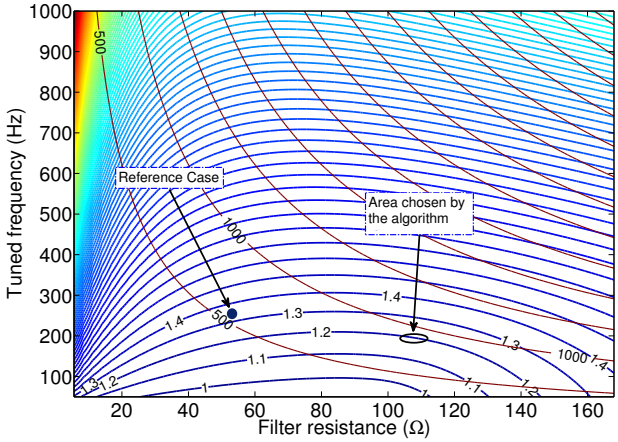

Fig. 14. Filter design graph for the CRL filter. The set of parameters the algorithm has chosen are limited by the 1.2 contour line and the maximum filter impedance along this line.

4) Medium Voltage LCR Filter (MV LCR)

The block diagram for the MV LCR filter is given in Fig. 9. The inductor value is kept constant during the analysis at maximum (0.15pu). The maximum value of inductance is set to be 0.15pu because a very large series inductance can reduce the capability of the generator to produce rated torque. The filter design graph for the MV LCR filter is given in Fig. 15.

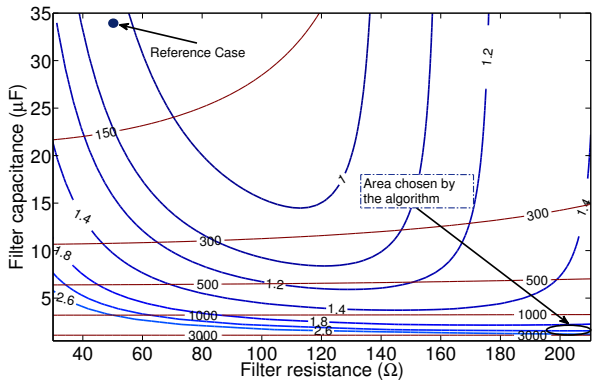

Fig. 15. Filter design graph for the MV LCR filter. The set of parameters the algorithm has chosen are limited by the 2.6 contour line and the maximum filter impedance along this line.

5) Low Voltage LCR Filter (LV LCR)

The block diagram for the LV LCR filter is given in Fig. 10. The inductor value is kept constant during the analysis at maximum. The filter design graph for the LV LCR filter is given in Fig. 16.

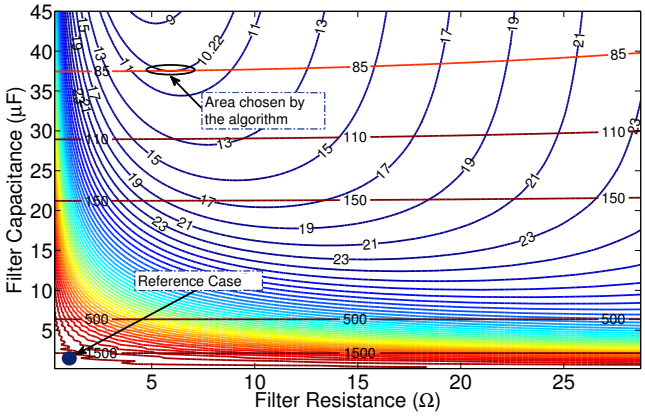

Fig. 16. Filter design graph for the LV LCR filter. The set of parameters the algorithm has chosen are limited by the 10.22 contour line and the maximum filter impedance along this line.

6) Combination of Filters

An additional advantage of the proposed algorithm is that it can take into account a combination of filters when determining the parameters for overvoltage mitigation. For example, additional harmonics are generated around the switching frequency of the controller. In order to reduce these harmonic components a single tuned filter can be used. The proposed algorithm can take into account the effect of the single tuned filter and calculate the parameters for the filter so that overvoltages are mitigated and losses are the least possible. A combination of a single tuned filter with a LV LCR filter is chosen and shown in Fig. 17.

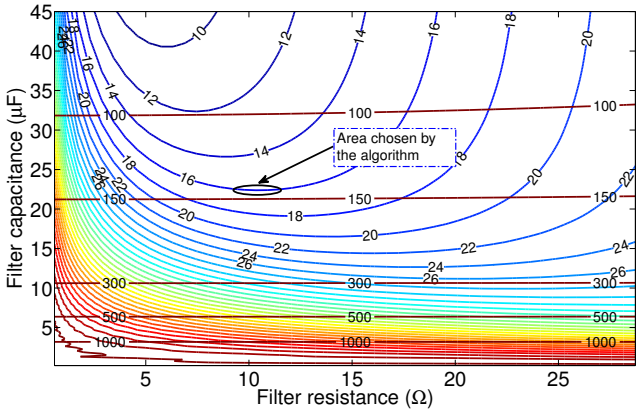

Fig. 17. Filter design graph for the LV LCR filter and single tuned filter.

Table II gives a summarized view of the filter parameters, chosen peak voltage gain from the design graph and filter impedance for all the types of filters considered.

TABLE II
FILTER PARAMETERS CHOSEN USING PROPOSED ALGORITHM

Filter type	Filter Parameters	Peak voltage gain	Filter impedance
R	R_f = 148.35 Ω	1.1809	148.35 Ω
CR	R_f = 111.96 Ω C_f = 4.991 μF	1.1995	647.26 Ω
CRL	R_f = 111.96 Ω L_f = 192.6 mH C_f = 3.842 μF	1.1922	867.79 Ω
MV LCR	R_f = 210.28 Ω L_f = 11.3 mH C_f = 1.132 μF	2.6716	2820.21 Ω
LV LCR	R_f = 5.746 Ω L_f = 0.2728 mH C_f = 37.501 μF	10.2242	85.08 Ω
LV LCR and Single Tuned	R_f = 10.35 Ω L_f = 0.2728 mH C_f = 22.50 μF	15.9989	141.85 Ω

VI. RESULTS AND DISCUSSION

In this section we will present the simulation results acquired for the different filter cases presented. As it was noted in section III, two different scenarios will be considered. The first scenario, which is the worst case scenario, will assume that the reflection coefficient at the generator terminals is unity, Γ_{Gen} = 1. The second scenario assumes that the reflection coefficient at the generator terminals is Γ_{Gen} = 0.5. Different cases regarding the generator reflection coefficient can also be considered however, this paper considers two cases as representatives to show the effect of changing the Γ_{Gen}.

A. *Worst case scenario: Γ_{Gen} = 1*

The results from simulating the proposed TCCS under all the cases discussed above are given in Table III.

First of all, a comparison is made between the efficiency of the proposed algorithm to derive the filter parameters in each case. Based on the results of Table III, we can observe that in all cases the proposed filters have fewer losses from the filter created using reference parameters. In addition, all the proposed filters are able to limit overvoltages at the generator terminals below 1.2pu, the highest overvoltage being 1.1659pu. This is not the case for reference filters; the LV LCR filter has a peak overvoltage above 1.2pu which can lead to insulation damage at the generator. It should be noted that the equations to calculate the reference filter parameters were derived for a machine-cable-converter system whereas the TCCS in this paper also includes a transformer.

TABLE III
COMPARISON OF FILTER DESIGN METHODS FOR THE WORST CASE SCENARIO

Filter type	Filter Design Method	Peak overvoltage (pu)	Filter Losses (%P_{Gen})	System Total Losses (%P_{Gen})
R	Reference	1.0097	56.11	57.15
	Proposed	1.1375	21.89	24.25
CR	Reference	1.1877	3.91	8.02
	Proposed	1.1659	1.74	5.68
CRL	Reference	1.1709	4.32	8.01
	Proposed	1.1303	1.31	4.81
MV LCR	Reference	1.0611	14.32	17.5
	Proposed	1.0601	0.17	3.72
LV LCR	Reference	2.4563	0.35	4.02
	Proposed	1.1231	0.23	4.23
LV LCR and Single Tuned	Proposed	1.0411	0.15	4.07

Taking a closer look at the losses from the filters we can see that the minimum losses are generated by the proposed MV LCR filter and the LV LCR in combination with single tuned filter. In addition to the very low losses, the maximum overvoltage at the generator terminals for these types of filters is close to 1pu which means that voltage reflections and harmonic resonance are mitigated effectively. As it is expected, the proposed MV LCR filter and the LV LCR in combination with single tuned filter also have the minimum total system losses compared to the rest of the filters, up to 0.5% less losses from the proposed LV LCR filter. A possible disadvantage of the proposed MV LCR filter is that the components have to withstand medium voltage and this can increase the capital cost of the filter. The proposed LV LCR filter in combination with a single tuned filter operates onshore, at low voltage, has the lowest voltage total harmonic distortion (VTHD) and generates minimum losses making such combination favorable for a TCCS.

Regarding the offshore filters we can observe that the R-filter generates very high losses and so this type cannot be considered an option. The proposed CR-filter and CRL-filter generate an acceptable amount of losses for TCCS, 1.74% and 1.31% respectively. Generally, offshore filters have to operate underwater and also generate higher losses compared to onshore filters making their use in a TCCS unlikely.

B. *Second scenario: Γ_{Gen} = 0.5*

The results from simulating the proposed TCCS under the second scenario are given in Table IV.

TABLE IV
COMPARISON OF FILTER DESIGN METHODS FOR THE SECOND SCENARIO

Filter type	Filter Design Method	Peak overvoltage (pu)	Filter Losses (%P_{Gen})	System Total Losses (%P_{Gen})
R	Reference	1.0001	56.09	57.12
	Proposed	1.0575	21.79	24.12
CR	Reference	1.1471	3.88	7.98
	Proposed	1.0935	1.72	5.64
CRL	Reference	1.1012	4.29	7.96
	Proposed	1.0678	1.27	4.76
MV LCR	Reference	1.0450	14.29	17.15
	Proposed	1.0411	0.17	3.71
LV LCR	Reference	1.5032	0.34	4.05
	Proposed	1.0014	0.21	4.19
LV LCR and Single Tuned	Proposed	1.0091	0.15	4.16

As an overall observation it can be said that filter losses are not significantly affected when Γ_{Gen} changes. In addition, peak overvoltages are lower for both design methods. However, in the reference case of the LV LCR filter we can see that peak overvoltage is above 1.2pu even though it is much lower compared to the worst case scenario. As for the rest of the filters the trends are similar to the worst case scenario. Offshore filters generate very high losses and their use in a TCCS is unlikely. The least possible losses are generated by the proposed MV LCR filter and the combination of LV LCR filter with a single tuned filter. The fact that peak overvoltages are much lower is very important since the second scenario is more realistic compared to the worst case scenario. Therefore, using the worst case scenario we can design filters taking into account the limits of the system but in reality the system will operate under more favorable conditions.

C. *Simulated operation*

In Fig. 18 the comparison of generator voltages between the reference and proposed filters of LV LCR and MV LCR are depicted.

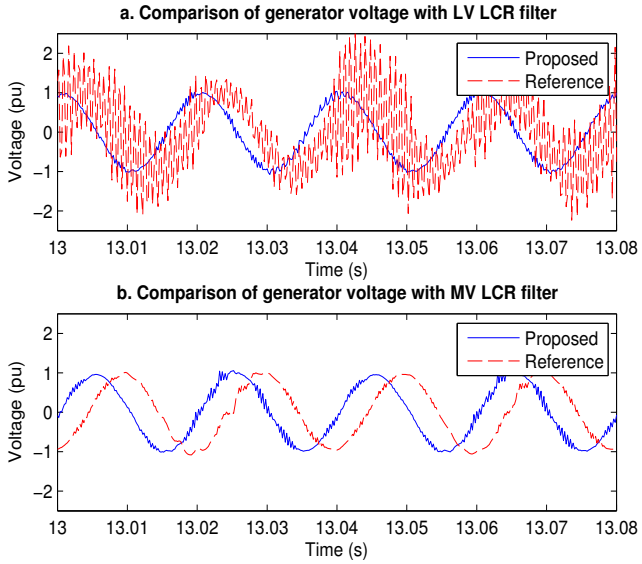

Fig. 18. Comparison of generator voltages for proposed and reference filter design for (a) LV LCR filter and (b) MV LCR filter.

It can be seen that in the reference case of the LV LCR filter the voltage exceeds the 1.2pu limit. Using the proposed parameters for the LV LCR filter the overvoltages are limited. In the case of the MV LCR filter both cases have low overvoltages near 1pu. However the filter of the proposed case generates significantly lower losses as given in Tables III and IV.

In Fig. 19 the flow speed, active power, pitch angle and generator speed can be seen for 70 minutes of operation. The proposed LV LCR filter was used.

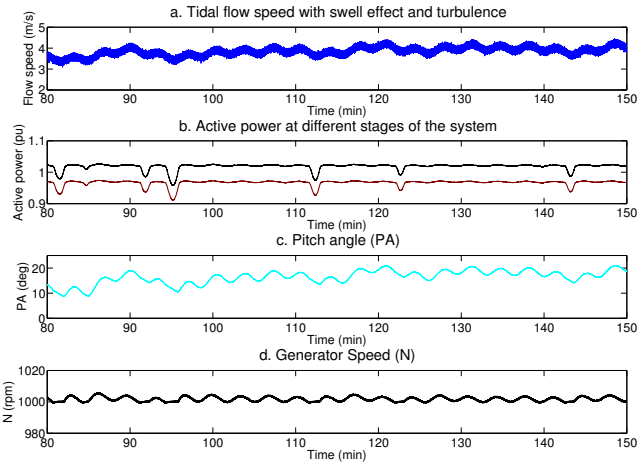

Fig. 19. Tidal flow speed, active power, pitch angle and generator speed for the TCCS with the proposed LV LCR filter.

As noted in section IV the TCCS was studied in high tidal flow speeds in order to study filter design under rated operation. In Fig. 19 we can observe the power from the generator that fluctuates at some instances due to the sudden changes of the tidal flow speed but overall active power is kept close to 1pu due to the pitch angle control.

VII. CONCLUSIONS

In this paper we propose an electrical configuration for a TCCS with onshore converters. This configuration is based on generator-cables-transformer-converter interaction which is advantageous for small distances. It offers reduced operation and maintenance requirements for the power electronics and control of the transmission voltage for reduced transmission losses. A key contribution of the paper is the description, modeling and system design of a resource-to-grid TCCS with long distance controls. In addition, we calculate the parameters for different types of literature-based filters. The major contribution of this paper is the development of an algorithm to calculate filter parameters so that installed filters both mitigate overvoltages and generate the least possible losses. In all cases the proposed algorithm was able to generate a set of filter parameters that results in fewer losses and a peak overvoltage below the limits. Based on the results from the algorithm both the MV LCR filter and LV LCR filter are possible solutions in a TCCS. The filter design process based on the proposed algorithm can be used for systems with a similar electrical configuration and its application is not limited to TCCS.

APPENDIX

TABLE V
GENERATOR PARAMETERS

Quantity	Value
Nominal Voltage (V)	6600
Frequency (Hz)	50
Stator resistance (pu)	0.00548
Stator inductance (pu)	0.08716
Rotor resistance (pu)	0.00399
Rotor inductance (pu)	0.08915
Mutual Inductance (pu)	3.99779
Rotor inertia (kg.m^2)	90
Pole pairs	3

TABLE VI
DC LINK PARAMETERS

Quantity	Value
DC Link Voltage (V)	1100
DC Link capacitance (mF)	11.6
Inverter nominal line voltage (V)	690

REFERENCES

[1] Department of Energy and Climate Change. 2014, July. UK ENERGY IN BRIEF 2014. A National Statistics Publication. Available: https://www.gov.uk/government/statistics/uk-energy-in-brief-2014

[2] F. Spinato, P. J. Tavner, G. J. W. van Bussel, and E. Koutoulakos, "Reliability of wind turbine subassemblies," *IET Renew. Power Gener.*, vol. 3, no. 4, p. 387, 2009.

[3] A. von Jouanne, D. A. Rendusara, P. N. Enjeti, and J. W. Gray, "Filtering techniques to minimize the effect of long motor leads on PWM inverter-fed AC motor drive systems," *IEEE Trans. Ind. Appl.*, vol. 32, no. 4, Jul./Aug., pp. 919–926, 1996.

[4] A. von Jouanne and P. Enjeti, "Design considerations for an inverter output filter to mitigate the effects of long motor leads in ASD applications," *IEEE Trans. on Ind. Applicat.*, vol. 33, no. 5, pp. 1138–1145, 1997.

[5] R. M. Tallam, G. L. Skibinski, T. A. Shudarek, and R. A. Lukaszewski, "Integrated Differential-Mode and Common-Mode Filter to Mitigate the Effects of Long Motor Leads on AC Drives," *IEEE Trans. on Ind. Applicat.*, vol. 47, no. 5, pp. 2075–2083, Sep. 2011.

[6] A. K. Abdelsalam, M. I. Masoud, S. J. Finney, and B. W. Williams, "Vector control PWM-VSI induction motor drive with a long motor feeder: performance analysis of line filter networks," *IET Electr. Power Appl.*, vol. 5, no. 5, p. 443, 2011.

[7] A. F. Moreira, T. A. Lipo, G. Venkataramanan, and S. Bernet, "High-frequency modeling for cable and induction motor over voltage studies in long cable drives," *IEEE Trans. Ind. Appl.*, vol. 38, no. 5, pp. 1297–1306, Sep.-Oct. 2002.

[8] B. Gustavsen, "Study of Transformer Resonant Overvoltages Caused by Cable-Transformer High-Frequency Interaction," *IEEE Trans. Power Delivery*, vol. 25, no. 2, pp. 770–779, Apr. 2010.

[9] J. Rodriguez, J. Pontt, C. Silva, R. Musalem, P. Newman, R. Vargas, and S. Fuentes, "Resonances and overvoltages in a medium-voltage fan motor drive with long cables in an underground mine," *IEEE Trans. Ind. Appl.*, vol. 42, no. 3, pp. 856–863, May/Jun. 2006.

[10] M. Kuschke and K. Strunz, "Transient Cable Overvoltage Calculation and Filter Design: Application to Onshore Converter Station for Hydrokinetic Energy Harvesting," *IEEE Trans. Power Delivery*, vol. 28, no. 3, pp. 1322–1329, Jul. 2013.

[11] B. Whitby and C. Ugalde-Loo, "Performance of Pitch and Stall Regulated Tidal Stream Turbines," *IEEE Trans. Sustain. Energy*, vol.5, no.1, pp.64,72, Jan. 2014.

[12] S. Benelghali, M. E. H. Benbouzid, J. F. Charpentier, T. Ahmed-Ali, and I. Munteanu, "Experimental Validation of a Marine Current Turbine Simulator: Application to a Permanent Magnet Synchronous Generator-Based System Second-Order Sliding Mode Control," *IEEE Trans. Ind. Electron.*, vol. 58, no. 1, pp. 118–126, Jan. 2011.

[13] F. Mekri, S. Ben Elghali, and M. E. H. Benbouzid, "Fault-Tolerant Control Performance Comparison of Three- and Five-Phase PMSG for Marine Current Turbine Applications," *IEEE Trans. Sustain. Energy*, vol. 4, no. 2, pp. 425–433, Apr. 2013.

[14] S. E. Ben Elghali, M. E. H. Benbouzid, T. Ahmed-Ali, and J. F. Charpentier, "High-Order Sliding Mode Control of a Marine Current Turbine Driven Doubly-Fed Induction Generator," *IEEE J. Oceanic Eng.*, vol. 35, no. 2, pp. 402–411, Apr. 2010.

[15] Z. Zhou, F. Scuiller, J. F. Charpentier, M. E. H. Benbouzid, and T. Tang, "Power Smoothing Control in a Grid-Connected Marine Current Turbine System for Compensating Swell Effect," *IEEE Trans. Sustain. Energy*, vol. 4, no. 3, pp. 816–826, Jul. 2013.

[16] S. E. Ben Elghali, M. E. H. Benbouzid, and J. F. Charpentier, "Modelling and control of a marine current turbine-driven doubly fed induction generator," *IET Renew. Power Gener.*, vol. 4, no. 1, p. 1, 2010.

[17] M. C. Sousounis, J. K. H. Shek, and M. A. Mueller, "Modelling and control of a Tidal Energy Conversion system with long distance converters," Power Electronics, Machines and Drives (PEMD 2014), 7th IET International Conference on, pp.1,6, 8-10 April 2014.

Marios C. Sousounis received the Diploma in electrical engineering and computer science from the National Technical University of Athens, Athens, Greece, in 2011, the M.Sc. in Sustainable energy systems from the University of Edinburgh, Edinburgh, UK, in 2012.

He is currently pursuing the Ph.D. degree in electrical engineering at the University of Edinburgh, Edinburgh, UK. His research interest includes, fault tolerant control, optimization of offshore renewables and tidal energy integration.

Jonathan K. H. Shek received M.Eng(Hons) and Ph.D degrees from the University of Edinburgh, Edinburgh, UK, in 2004 and 2009 respectively.

He was a postdoctoral researcher from 2009 to 2012 working in the area of power take-off, condition monitoring and control for renewable energy devices. Dr Shek currently holds the position of Chancellor's Fellow within the Institute for Energy Systems at the University of Edinburgh. His main research interest lies in power electronics and control, particularly its application in sustainable energy systems, such as renewable energy and electric vehicles.

Markus A. Mueller received the B.Sc.(Eng.) degree in electrical and electronic engineering from Imperial College London, London, U.K., in 1988 and the Ph.D. degree in electrical engineering from the University of Cambridge, Cambridge, U.K., in 1991.

He was a Lecturer with the School of Engineering and Computing Sciences, University of Durham, Durham, U.K. Since January 2004, he has been with the School of Engineering, The University of Edinburgh, Edinburgh, U.K., where he has been a Personal Chair in Electrical Machines since August 2012 and is Head of the Institute for Energy Systems. In 2009, he founded NGenTec Ltd. to commercialize a permanent-magnet generator for wind turbines. His research interests include the design and modeling of electrical machines for renewable energy converters.